

## Wave-Mean Flow Interaction during the Life Cycles of Baroclinic Waves

STEVEN B. FELDSTEIN

*Cooperative Institute for Research in the Environmental Sciences, University of Colorado, Boulder, Colorado*

(Manuscript received 4 March 1991, in final form 29 October 1991)

### ABSTRACT

A two-layer quasigeostrophic  $\beta$ -plane channel model is used to examine the role of the wave-mean flow interaction during the life cycles of baroclinic waves. Two cases are examined: a wide and a narrow jet limit. These two limits are required to satisfy the property that their instability lead to a realistic baroclinic life cycle consisting of baroclinic growth and barotropic decay. In order to characterize the properties of the zonal-wind tendency in the two cases, scaling arguments based on a study by Andrews and McIntyre are used. This scaling procedure is then used to explain the nonlocal (local) zonal-wind tendency during the realistic baroclinic life cycle for the wide (narrow) jet limit.

Several differences between the properties of the two jet limits are found. For the wide jet limit, the acceleration at the center of the jet is confined to the growth stage. This contrasts the narrow jet limit where the jet is accelerated throughout the entire life cycle. These differences depend upon the lower-layer potential vorticity fluxes, which exhibit the same timing properties as the zonal-wind tendency. In addition, for both the wide and narrow jet limits, irreversible potential vorticity mixing is shown to force nonlocal and local permanent changes to the zonal wind, respectively. A comparison is also made between the vorticity flux and potential vorticity flux to determine which is a better predictor of the zonal-wind tendency. It is shown that in the wide (narrow) jet limit, the vorticity (potential vorticity) flux does better at predicting the zonal-wind tendency. It is also argued that one can use a barotropic model to study the temporal evolution of the upper-layer flow for both the narrow and wide jet limits.

Last, it is shown that the properties of the inviscid calculations are retained when thermal forcing and surface Ekman friction are included. Calculations are performed with different values for the surface Ekman friction coefficient and with the thermal forcing coefficient fixed. For the wide (narrow) jet limit, it is found that the disturbance grows to a larger (smaller) total energy as the Ekman friction coefficient is increased (decreased). This behavior for the wide jet limit is explained in terms of an enhancement of the baroclinic energy conversions that overcome the barotropic governor mechanism of James and Gray.

### 1. Introduction

An examination of daily weather maps shows that the properties of the midlatitude westerly jet are extremely variable. In particular, one can see large changes in its strength, position, and width. Because of the interaction of synoptic-scale waves with the midlatitude westerly jet, synoptic-scale baroclinic waves must also exhibit large variability in their life cycles [as an example of this variability in the Southern Hemisphere see Randel and Stanford (1985a)]. One fruitful approach for studying the interaction between synoptic-scale baroclinic waves with the background westerly zonal flow during baroclinic life cycles has been to use idealized models with a zonally symmetric initial zonal flow. Examples of different techniques that have been employed for studying this problem include the analytical weakly nonlinear two-layer quasigeostrophic models of Pedlosky (1970, 1971, 1980, 1981)

and the numerical multilevel primitive equation models of Simmons and Hoskins (1978, 1980).

In two previous studies, Feldstein and Held (1989) and Feldstein (1991) (FH and F, respectively, hereafter), the life cycles of baroclinic waves were examined with a two-layer quasigeostrophic model. In these studies, it was found that if the meridional shear in the upper-layer zonal wind is sufficiently strong to produce a critical latitude, the disturbance undergoes a life cycle of baroclinic growth followed by barotropic decay that resembles those life cycles observed in the atmosphere (see Randel and Stanford 1985a,b). Because of its success in reproducing many of the dominant features of the baroclinic life cycle seen in the atmosphere, the same two-layer quasigeostrophic model as in FH and F will be used to investigate the effect of different jet widths on the properties of the wave-mean flow interaction during the baroclinic life cycles. The approach to be adopted is to examine two limiting cases, one with a very wide jet and the other with a very narrow jet. In this manner, fundamental properties of the wave-mean flow interaction can be isolated.

A brief description of the model is presented in sec-

---

*Corresponding author address:* Dr. Steven B. Feldstein, University of Colorado, Cooperative Institute for Research in the Environmental Sciences, Campus Box 449, Boulder, CO 80309-0449.

tion 2. The life-cycle solutions with an emphasis on the properties of the wave-mean flow interaction are shown in section 3. In section 4, the results with surface Ekman friction and thermal forcing are presented. The conclusions appear in section 5.

## 2. Model description

A detailed description of the model including the boundary conditions can be found in FH. The streamfunction  $\psi$  and the potential vorticity  $q$  are separated into a zonally averaged and a disturbance part:

$$\begin{aligned}\psi_n(x, y, t) &= \Psi_n(y, t) + \psi'_n(x, y, t) \\ q_n(x, y, t) &= Q_n(y, t) + q'_n(x, y, t),\end{aligned}\quad (1)$$

where  $n = 1$  denotes the upper layer and  $n = 2$  the lower layer, and  $\psi_n$  and  $q_n$  are related by

$$q_n = \nabla^2 \psi_n + \beta y + (-1)^n (\psi_1 - \psi_2)/2. \quad (2)$$

The dimensionless disturbance and zonally averaged potential vorticity equations are

$$\partial q'_n / \partial t + U_n \partial q'_n / \partial x + v'_n \partial Q_n / \partial y = -\nu \nabla^6 \psi'_n; \quad (3)$$

and

$$\partial Q_n / \partial t = -\partial(\overline{v'_n q'_n}) / \partial y - \nu \nabla^6 \Psi_n. \quad (4)$$

For the two-layer quasigeostrophic model, the equations relating the zonally averaged zonal flow to the zonally averaged potential vorticity flux can be derived by combining the equations for the zonal-wind tendency  $\partial U_n / \partial t$  and potential temperature tendency  $\partial \theta / \partial t$

$$\partial U_n / \partial t = \overline{v'_n q'_n} + \bar{v}_n^* + \nu \partial^4 U_n / \partial y^4 \quad (5a)$$

$$\partial \theta / \partial t = -\bar{w}^*, \quad (5b)$$

where

$$\begin{aligned}\bar{v}_n^* &= \bar{v}_n - (-1)^n \overline{v'_1 \theta'} \\ \bar{w}^* &= \bar{w} + \partial(\overline{v'_1 \theta'}) / \partial y,\end{aligned}\quad (6a)$$

$$\bar{w}^* = 1/2(\partial \bar{v}_1^* / \partial y), \quad (6b)$$

and  $\theta' = \psi'_1 - \psi'_2$ , to give

$$\begin{aligned}\partial / \partial t (\partial^2 U_n / \partial y^2 - 2U_n) &= \partial^2 \overline{v'_n q'_n} / \partial y^2 \\ &- (\overline{v'_1 q'_1} + \overline{v'_2 q'_2}) - \nu \nabla^4 (\partial^2 U_n / \partial y^2 - 2U_n).\end{aligned}\quad (7)$$

In this study, the initial jet profile is given the form

$$U_1(y, 0) = \text{sech}^2[(y - y_0)/\sigma]; \quad U_2(y, 0) = 0, \quad (8)$$

where  $y_0 = 0.5W$ ,  $W$  being the width of the channel and  $\sigma$  the half-width of the jet:  $U_1(y, 0)$  has been scaled so that it has a value of 1.0 in the center of the channel and  $W$  will always be large enough so that  $U_1$  goes to a value very close to zero before the channel walls.

## 3. Life cycles

In this section, we will examine the wave-mean flow interaction during the baroclinic life cycles for two cases: a “wide jet” and a “narrow jet” limit. For these calculations, the initial jet will be weakly supercritical to instability. As in F, a weakly supercritical initial state is chosen since the results are simpler and easier to interpret. Also, as in F, the disturbance is limited to one zonal wavenumber since the solution is not found to be sensitive to the zonal truncation. Before proceeding to look at the numerical solution, it is necessary to define the wide and narrow jet limits for the present problem. This definition is based on the constraint that the instability of this jet must lead to a life cycle characterized by baroclinic energy conversions from the zonal flow to the disturbance during the growth stage and by barotropic energy conversions from the disturbance back to the zonal flow during the decay stage, as is typically observed in the atmosphere. In F, it was found that if the jet was sufficiently wide, the energy conversions between the disturbance and the zonal flow are baroclinic in both the growth and decay stages. Therefore, the wide jet limit is defined to be approximately the widest possible jet for which the energy conversions are barotropic while the disturbance is decaying. On the other hand, the narrow jet limit is defined as approximately the narrowest possible jet for which the upper-layer meridional potential vorticity gradient, that is,  $\partial Q_1 / \partial y$ , is initially positive and remains positive throughout the life cycle. In that way, barotropic energy conversions cannot contribute to the growth of the disturbance.

This concept of wide and narrow jet limits is closely related to scaling of the zonal-mean flow by Andrews and McIntyre (1976). In that study, a “tall” mean flow was defined as one in which the ratio  $fL/NH \ll 1$  where  $f$  is the Coriolis parameter,  $N$  the Brunt-Väisälä frequency,  $L$  the horizontal length scale, and  $H$  the vertical length scale. Under these conditions, they showed that the response to the wave forcing, that is, the meridional potential vorticity flux, is *local*, and the eddy-induced residual circulation is negligible. As a result, the tendency equation for the zonal-mean flow in a vertically continuous flow becomes  $\partial U / \partial t = \overline{v'_n q'_n}$ . Although not discussed by Andrews and McIntyre, if one examines the opposite case where  $fL/NH \gg 1$ , it is straightforward to show that the tendency of the zonal-mean flow is barotropic, that is,  $\partial / \partial t (\partial U / \partial z) = 0$ , where  $z$  is the vertical length coordinate. This implies that even if the meridional potential vorticity flux varies with height, the zonal-flow response must be *nonlocal* as a residual circulation must be induced to maintain the barotropic zonal-flow tendency.

In the continuous case of Andrews and McIntyre, the four parameters that comprise the ratio  $fL/NH$  determine the appropriate balance in the zonal-wind

tendency equation, whereas in the present two-layer model, the only parameter that is being allowed to vary is the jet width  $\sigma$ . For the two-layer model, we can apply analogous scaling arguments to those of Andrews and McIntyre for both the wide and narrow jet limits by either neglecting or retaining the  $y$  derivative terms in (7), respectively. As a result, the wide and narrow jet zonal-wind tendency equations become

$$\partial U_n / \partial t = 1/2(\overline{v'_1 q'_1} + \overline{v'_2 q'_2}) \quad (9)$$

and

$$\partial U_n / \partial t = \overline{v'_n q'_n} + \nu \partial^4 U_n / \partial y^4, \quad (10)$$

respectively. These equations exhibit the same properties as in the continuous case.

#### a. Wide jet limit ( $\sigma = 16.0$ )

For the wide jet limit, we choose  $\sigma = 16.0$ ,  $\beta = 0.486$ ,  $W = 110.0$ ,  $\nu = 0.01$ ,  $k = 0.82$ , and 100 grid points in the meridional direction are used. The initial disturbance is chosen to be symmetric about the center of the jet (the fastest-growing normal mode is always found to be symmetric) and its amplitude is small enough so that it can attain its normal-mode form before modifying the zonal flow. The linear growth rate of this disturbance is  $\omega_i = 0.016$ .

The energy cycle is illustrated in Fig. 1. The disturbance undergoes a single life cycle of baroclinic growth followed by barotropic decay. If one were to compare this life cycle with that for a slightly wider jet, for ex-

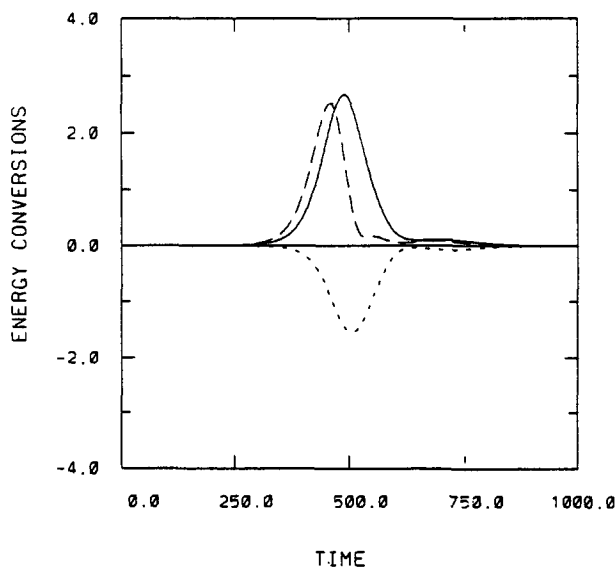


FIG. 1. Eddy energy (multiplied by  $2.0 \times 10^3$ ) and energy conversion (multiplied by  $1.0 \times 10^5$ ) for the wide limit  $\sigma = 16.0$  westerly jet. Solid line denotes total disturbance energy; long dashed line, baroclinic conversion; short dashed line, barotropic conversion.

ample,  $\sigma = 17.0$ , slightly negative baroclinic energy conversions would be found as the disturbance is decaying. Thus, the baroclinic life cycle for the  $\sigma = 16.0$  jet represents the wide jet limit as defined earlier in this section.

In Figs. 2a and 2b, the temporal evolutions of  $\partial U_1 / \partial t$  and  $\partial U_2 / \partial t$  are illustrated with a contour diagram. As expected, based upon these scaling arguments, the pattern of the zonal-wind tendencies in the two layers are very similar. At the center of the jet, both  $\partial U_n / \partial t$  remain positive during the growth stage and are negligible during the decay stage. At the wings of the jet, both  $\partial U_n / \partial t$  are very small while the disturbance is growing and become strongly negative while it is decaying. Thus, we get a simple picture of acceleration of the center of the jet during the growth stage and deceleration of the wings of the jet during the decay stage.

A further understanding of the zonal-wind tendencies can be attained by examining the temporal evolution of the potential vorticity fluxes (see Figs. 2c and 2d). In this case, if we compare the numerical values of the zonal-wind tendencies to those approximated by (9), the error is found to be about 20%. Therefore, for physical interpretation, (9) represents a good approximation (this is not surprising because the two  $\partial U_n / \partial t$  in Figs. 2a and 2b are similar). An inspection of Figs. 2c and 2d indicates that the lower-layer potential vorticity fluxes are dominant during the growth stage and the upper-layer potential vorticity fluxes are during the decay stage. This also allows one to arrive at the simple picture that the acceleration of the center of the jet in both layers is driven by the lower-layer potential vorticity flux and the deceleration of the wings of the jet in both layers is driven by the upper-layer potential vorticity flux. Furthermore, since the lower-layer potential vorticity flux is found to be very much dominated by the meridional heat flux, the jet can also be said to be accelerated by the meridional heat flux. Since the baroclinic energy conversion is equal to the integral of the product of the meridional heat flux with the vertical shear of the zonal wind, once the baroclinic growth ceases, so does the acceleration of the jet.

#### b. Narrow jet limit ( $\sigma = 1.5$ )

For the narrow jet limit, we choose  $\sigma = 1.5$ ,  $\beta = 0.39$ ,  $W = 15.0$ ,  $\nu = 5.0 \times 10^{-5}$ ,  $k = 0.82$ , and again use 100 grid points in the meridional direction. As in the wide jet limit, the amplitude of the initial disturbance is sufficiently small so that the zonal flow is not modified before the disturbance reaches normal-mode form. The linear growth of this disturbance is also  $\omega_i = 0.016$ .

The energy cycle is shown in Fig. 3. As in Fig. 1, the disturbance also undergoes a single life cycle of baroclinic growth and barotropic decay, but the time dif-

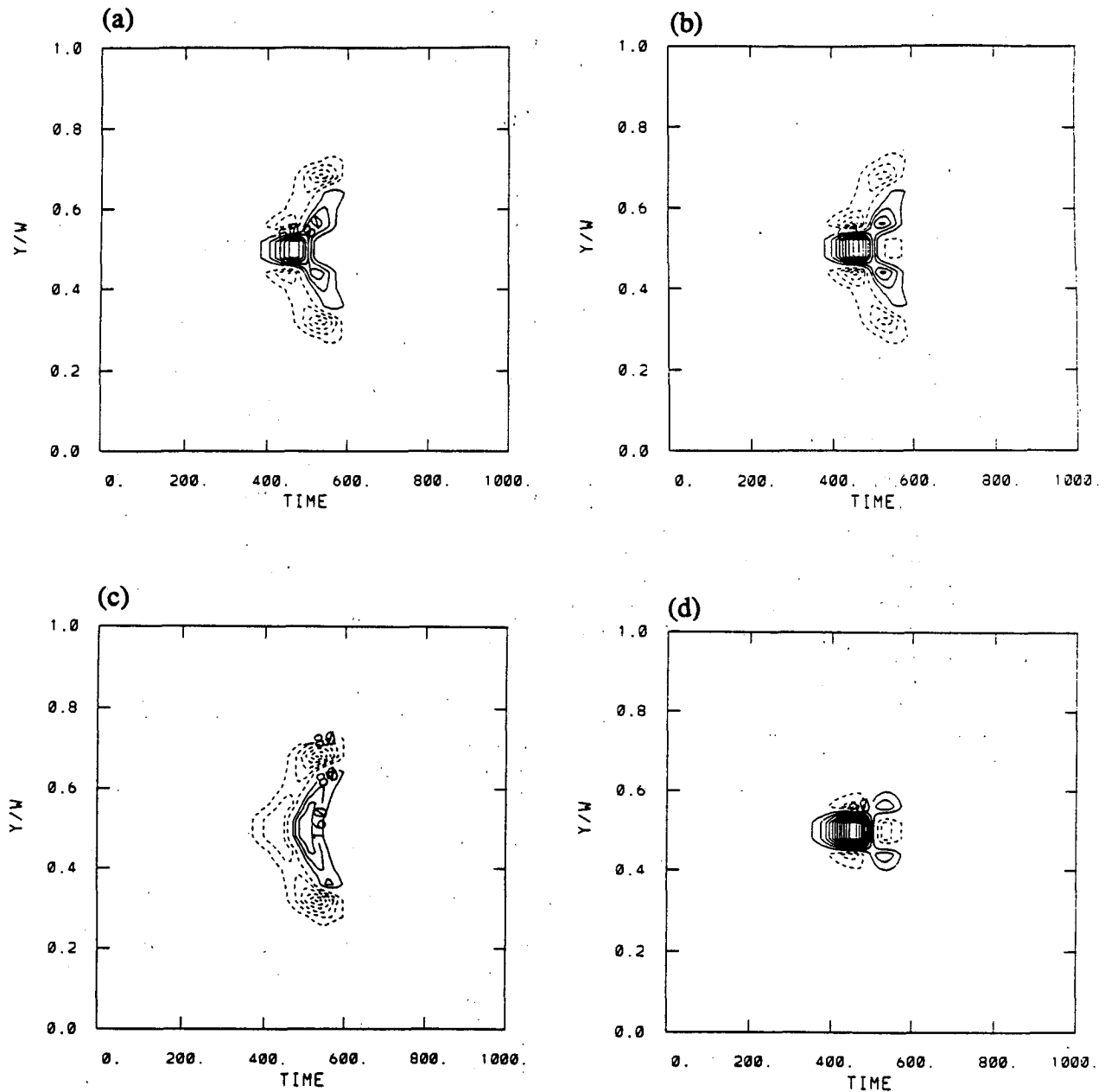


FIG. 2.  $y/W$ -time contour diagram of the tendency of the zonally averaged zonal wind and the upper- and lower-layer potential vorticity flux for the  $\sigma = 16.0$  westerly jet; (a)  $\partial U_1/\partial t$ , contour interval is  $6.0 \times 10^{-5}$ , (b)  $\partial U_2/\partial t$ , contour interval is  $6.0 \times 10^{-5}$ , (c)  $\overline{v_1'q_1'}$ , contour interval is  $8.0 \times 10^{-5}$ , (d)  $\overline{v_2'q_2'}$ , contour interval is  $8.0 \times 10^{-5}$ . Solid contours are positive and dashed contours negative.

ference between the maximum baroclinic and barotropic conversions is reduced. This behavior is discussed in F. A numerical calculation was also performed with  $\sigma = 1.25$  where it was found that although  $\partial Q_1/\partial y$  is initially positive everywhere, it becomes negative at a later stage of the life cycle. Thus, a  $\sigma = 1.5$  jet is an appropriate choice for our narrow jet limit.

The temporal evolution of the  $\partial U_n/\partial t$  are shown in Figs. 4a and 4b. These tendencies are dominated by an acceleration of the jet in the lower layer and deceleration of the wings of the jet in the upper layer. In addition, both the acceleration and deceleration occur throughout entire the life cycle. An understanding of the properties of the  $\partial U_n/\partial t$  can be obtained by examining the potential vorticity fluxes (see Figs. 4c and

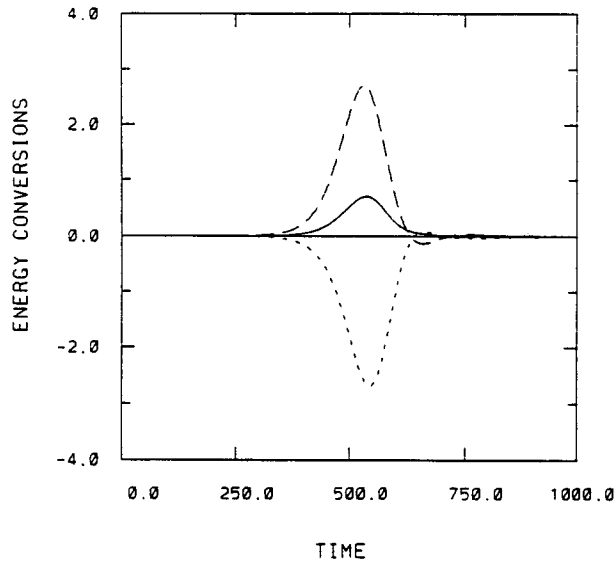


FIG. 3. As in Fig. 1 except for the narrow limit  $\sigma = 1.5$  jet.

4d) and then relating these fluxes to the zonal-wind tendencies through (10). Based on the scaling arguments that were used to derive (10), the zonal-wind response to the potential vorticity fluxes must be local so that the  $\partial U_n / \partial t$  and the  $\overline{v'_n q'_n}$  should bear a close resemblance. A comparison between  $\partial U_n / \partial t$  and  $\overline{v'_n q'_n}$  shows that the two patterns are similar, as the potential vorticity fluxes are concentrated in the same regions as  $\partial U_n / \partial t$ , but the accuracy of this approximation is not as good as the approximation made in the wide jet limit. In some sense, it is a surprising that the narrow jet approximation is even this good when one considers that the derivation of (10) required that the horizontal length scale be much less than one. Because the correspondence between the location of the potential vorticity fluxes and the zonal-wind tendencies are consistent with the properties implied by (10), the acceleration of the jet in the lower layer must be driven by the lower-layer potential vorticity flux and the deceleration of the wings of the jet in the upper layer must be driven by the upper-layer potential vorticity flux. The same property also shows that the absence of a significant zonal-wind acceleration (deceleration) at the center (wings) of the jet in the upper (lower) layer is because of the weak potential vorticity flux in these regions. It is also interesting to note that the weak upper-layer potential vorticity flux, and hence the small upper-layer zonal-wind acceleration at the jet center, occurs because of the strong cancellation between the upper-layer vorticity and heat flux that tends to occur in narrow jets. Furthermore, because of the relationship between the baroclinic energy conversion and the lower-layer potential vorticity flux, the acceleration of the jet in the lower layer must persist throughout the

life cycle together with the baroclinic energy conversion.

### c. Comparison between wide and narrow jet limits

There are several obvious differences that are apparent between the wide and narrow jet limits. It is verified that the scaling arguments, which were based on the scaling procedure of Andrews and McIntyre for the "tall" mean-flow condition, hold for the wide and narrow jet limits; within these limits, the zonal-flow response to the potential vorticity flux forcing is either nonlocal or local, respectively. We also saw differences in the timing of the acceleration in the center of the jet. For the wide jet limit, this acceleration was confined to the growth stage, whereas for the narrow jet limit, the acceleration of the jet occurred throughout the life cycle. These differences can be explained by noting that in both limits it is the lower-layer potential vorticity flux that forces the jet. In the wide jet limit,  $\overline{v'_2 q'_2}$  becomes small once the disturbance starts to decay, whereas in the narrow jet limit  $\overline{v'_2 q'_2}$  remains significant throughout the life cycle (an explanation of the timing of these fluxes can be found in F).

Because permanent changes in the zonal flow can be related to irreversible potential vorticity mixing, that is, the nonacceleration theorem of Charney and Drazin (1961), we examine the time-averaged potential vorticity fluxes over the entire life cycle (see Fig. 5a and 5b). For both the wide and narrow jet limits, the pattern of the time-averaged potential vorticity fluxes are very similar. In the upper layer, the time-averaged potential vorticity fluxes show negative values at the wings of the jet and near-zero values at the center of the jet due to cancellation between the negative and the positive potential vorticity fluxes during the growth and decay stages, respectively. In the lower layer, the time-averaged potential vorticity fluxes are positive in the center of the channel and negligible elsewhere.

These regions of nonzero time-averaged potential vorticity fluxes were found to be locations of strong potential vorticity mixing (see FH). This mixing leads to the formation of a region of almost zero  $\partial Q_2 / \partial y$  in the center of the lower layer (the negative  $\partial Q_2 / \partial y$  region is removed by this process and the zonal flow is stabilized). Although not discussed in FH and F, as  $U_2$  increases from zero during the life cycle, critical latitudes form in the negative  $\partial Q_2 / \partial y$  region in the lower layer. In the upper layer, the negative potential vorticity fluxes also correspond to regions of potential vorticity mixing where the latitudinally radiating disturbance is absorbed by the zonal wind (contour diagrams illustrating this process are shown in FH). The time-averaged zonal-wind tendencies are shown in Figs. 5a and 5b. As expected from Figs. 2 and 4, significant differences are found between the  $\partial U_n / \partial t$  for the two

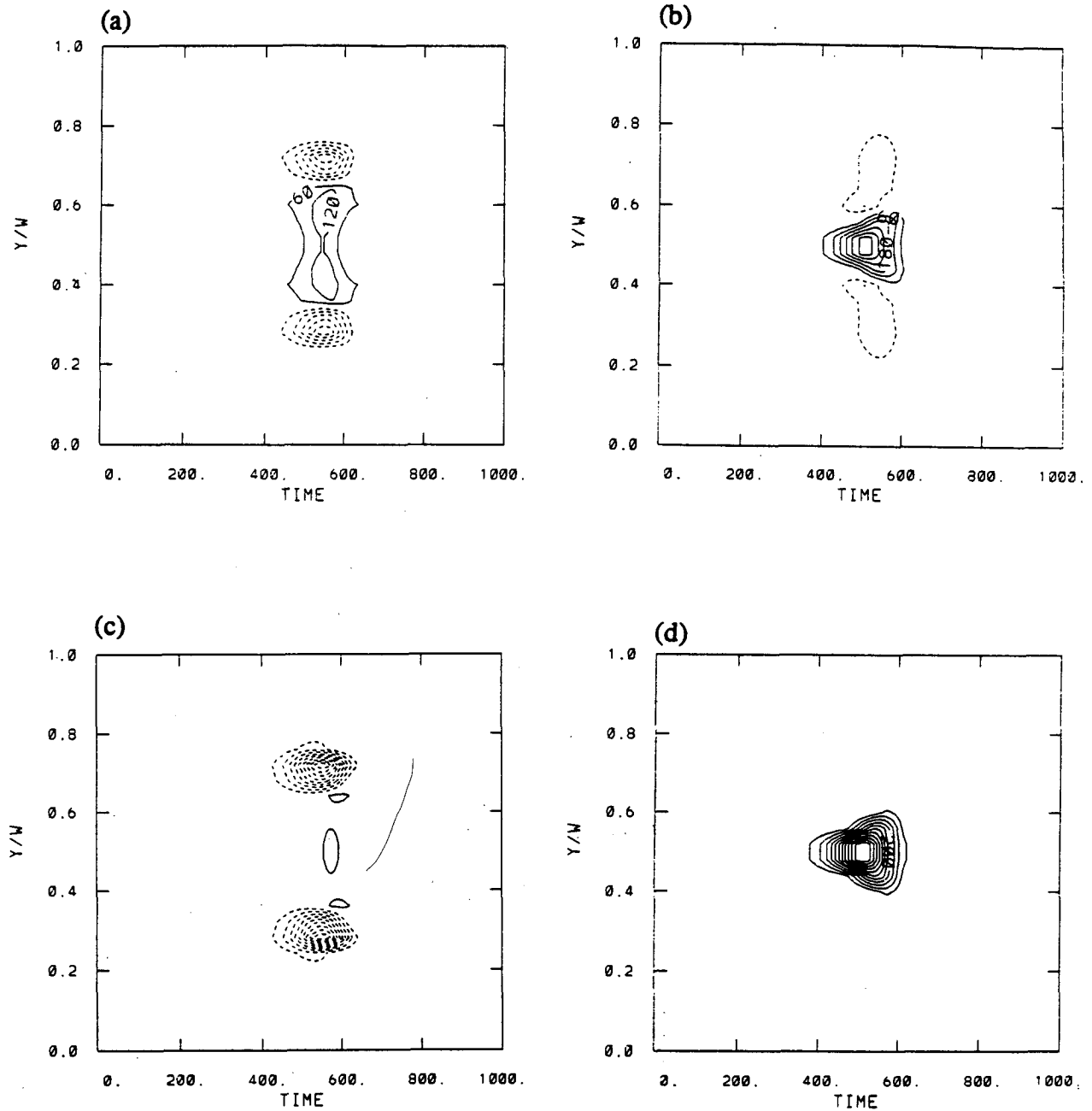


FIG. 4. As in Fig. 1 except for the narrow limit  $\sigma = 1.5$  jet; (a)  $\partial U_1/\partial t$ , contour interval is  $6.0 \times 10^{-5}$ , (b)  $\partial U_2/\partial t$ , contour interval is  $6.0 \times 10^{-5}$ , (c)  $v_1^2 q_1^2$ , contour interval is  $5.0 \times 10^{-5}$ . (d)  $v_2^2 q_2^2$ , contour interval is  $5.0 \times 10^{-5}$ .

limiting cases. The most obvious differences, consistent with earlier discussion, are the nonlocal versus local nature of the time-averaged zonal-wind tendencies in the wide and narrow jet limits. But, from Figs. 5a and 5b, we can see a close matching (much closer for the wide jet limit) in the location of nonzero time-averaged potential vorticity flux and zonal-wind tendency. Since the nonacceleration theorem requires that nonzero po-

tential vorticity fluxes cause changes to the zonal wind, we can directly relate the regions of potential vorticity mixing to that of the permanent zonal-wind changes.

This comparison between the wide and narrow jet limits yields some insight into whether the vorticity flux or the potential vorticity flux is a better predictor of the zonal-flow tendency. This particular problem was addressed by Pfeffer (1987), who examined the

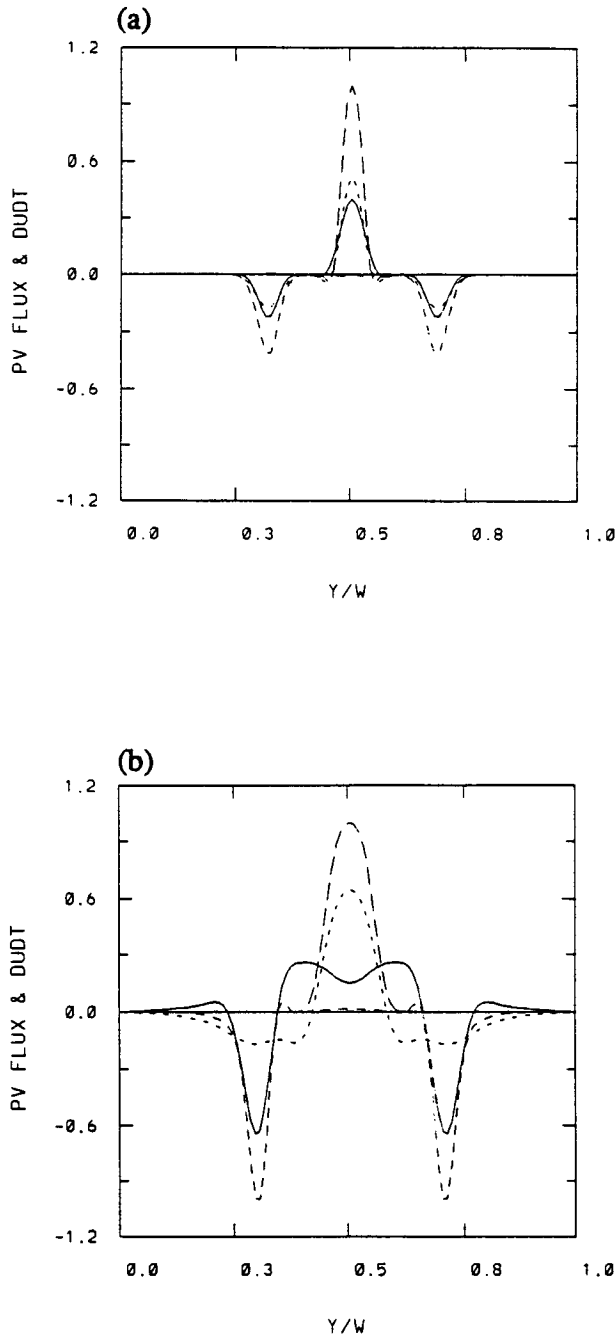


FIG. 5. Time-averaged zonal-wind tendency and potential vorticity flux for the (a)  $\sigma = 16.0$  and (b)  $\sigma = 1.5$  westerly jets. Solid line denotes  $\partial U_1/\partial t$ ; medium dashed line  $\partial U_2/\partial t$ ; short dashed line,  $\overline{v'_1 q'_1}$ ; long dashed line  $\overline{v'_2 q'_2}$ . These quantities are normalized by the maximum  $\overline{v'_2 q'_2}$ .

effect of the synoptic-scale transient eddies on the zonal-mean flow in the troposphere. He found that the pattern of the zonal-wind tendency has a better correlation with the vorticity flux than with the potential

vorticity flux. The same property is found in the wide jet limit in this study. This can be seen by referring to (9) and noting that  $\overline{v'_1 q'_1} + \overline{v'_2 q'_2} = \overline{v'_1 \zeta'_1} + \overline{v'_2 \zeta'_2}$  where  $\zeta'_n$  is the disturbance vorticity, and that  $\overline{v'_1 \zeta'_1} \gg \overline{v'_2 \zeta'_2}$ . This is not surprising since baroclinic life cycles with an initial zonal flow that resembles those seen in the climatological atmosphere have a strong nonlocal response (see Haynes and Shepherd 1989). On the other hand, if the jet is sufficiently narrow, as may sometimes occur in the troposphere for an instantaneous as opposed to a climatological zonal jet, the zonal-wind response may be better correlated with the potential vorticity flux and take on more local characteristics.

#### 4. Solutions with forcing and damping

In this section, we will examine the wave-mean flow interaction for both the wide and narrow jet limits with surface Ekman friction and thermal forcing present. When these two effects are included, the tendency equation for the zonal wind becomes

$$\begin{aligned} \partial/\partial t(\partial^2 U_n/\partial y^2 - 2U_n) &= \partial^2 \overline{v'_n q'_n}/\partial y^2 \\ &- (\overline{v'_1 q'_1} + \overline{v'_2 q'_2}) - \nu \nabla^4 (\partial^2 U_n/\partial y^2 - 2U_n) \\ &- (-1)^n (r_f U_2 - r_t (\partial\theta/\partial y - \partial\theta^*/\partial y)) \\ &- \delta_{n,2} r_f \partial^2 U_2/\partial y^2, \quad (11) \end{aligned}$$

where  $r_f$  and  $r_t$  are Ekman friction and thermal forcing coefficients and  $\delta_{n,2}$  is the Kronecker delta. If we follow the same scaling procedure as was used in deriving (9) and (10), the wide and narrow jet limits of (11) are

$$\begin{aligned} \frac{\partial}{\partial t} U_n &= \frac{1}{2} (\overline{v'_1 q'_1} + \overline{v'_2 q'_2}) \\ &+ \frac{1}{2} (-1)^n [r_f U_2 - r_t (\partial\theta/\partial y - \partial\theta^*/\partial y)] \quad (12) \end{aligned}$$

and

$$\frac{\partial}{\partial t} U_n = \overline{v'_n q'_n} - \nu \nabla^4 U_n - \delta_{n,2} r_f U_2, \quad (13)$$

respectively. In addition to the local versus nonlocal differences between (12) and (13), it is seen that thermal forcing is more important in the wide jet limit and surface friction acts to accelerate (decelerate) the lower-layer flow in the wide (narrow) jet limit.

A series of numerical integrations were performed with both surface Ekman friction and thermal forcing included. For both the wide and narrow jet limits, the thermal forcing coefficient is set at  $r_t = 0.002$ , and the Ekman friction coefficient is specified as either  $r_f = r_t$  or  $r_f = 10r_t$ . Linear stability analyses with this choice of parameters show that in the narrow jet limit the linear growth rate is very sensitive to the value of  $r_f$ ,

that is, for  $r_f = r_t$ ,  $\omega_i = 0.0138$  and for  $r_f = 10r_t$ ,  $\omega_i = 0.0050$ . When the linear stability analyses are performed for the wide jet limit, the linear growth rate is found to be insensitive to the value of  $r_f$ , that is, for  $r_f = r_t$ ,  $\omega_i = 0.0152$  and for  $r_f = 10r_t$ ,  $\omega_i = 0.0156$  (similar growth rates were also found for intermediate values of  $r_f$ ).

For both the wide and narrow jet limits, the corresponding nonlinear numerical integrations retained the nonlocal and local characteristics for the zonal-wind tendency, as discussed earlier. Furthermore, in the narrow jet limit for both values of  $r_f$ , and in the wide jet limit when  $r_f = r_t$ , the total energy of the disturbance vacillates toward a steady state. On the other hand, when  $r_f = 10r_t$  in the wide jet limit, after an initial transient stage, the disturbance undergoes periodic vacillations (the energy cycles for the wide jet limit are shown in Figs. 6a and 6b). In the narrow jet limit, consistent with the values of the linear growth rates, the total energy attained by the disturbance is smaller with the larger  $r_f$ . The wide jet limit solution shows the opposite behavior as it is the larger  $r_f$  that yields a significantly greater total energy. This behavior resembles that found in James and Gray (1986) where they show with a multilevel primitive equation model that the disturbance energy increases with a larger surface friction. Their explanation for this property (see also James 1987), which they call the barotropic governor, is that for smaller surface friction the disturbance becomes more meridionally confined. This is because the meridional shear of the zonal wind builds up as the disturbance grows and this enhanced shear causes the critical latitudes to move in toward the jet center. As a result, the disturbance is stabilized since the barotropic energy conversions become stronger.

In the present two-layer model, for both values of  $r_f$  in the wide jet limit, the temporal evolution of the phase speed of the disturbance was examined. For  $r_f = r_t$ , the disturbance phase speed  $c_r = 0.0138$  initially and increases to a value of  $c_r = 0.0212$  near its first total energy maximum after which it becomes slightly smaller. For  $r_f = 10r_t$ ,  $c_r = 0.034$  initially, but then increases substantially up to  $c_r = 0.103$  also at a time close to its first total energy maximum. In addition, the  $r_f = 10r_t$  solution exhibits a stronger zonal-wind increase (not shown) with greater meridional shear of the zonal wind. This suggests that the disturbance may be more meridionally confined in the  $r_f = 10r_t$  case, which is opposite to the behavior found by James and Gray. However, an examination of the temporal evolution of the potential vorticity fluxes (not shown) indicates that for both values of  $r_f$  the meridional extent of the disturbance is the same. This indicates that a mechanism other than that found by James and Gray (1986) for the primitive equation model must be responsible for the increase in disturbance energy with surface friction for the two-layer quasigeostrophic

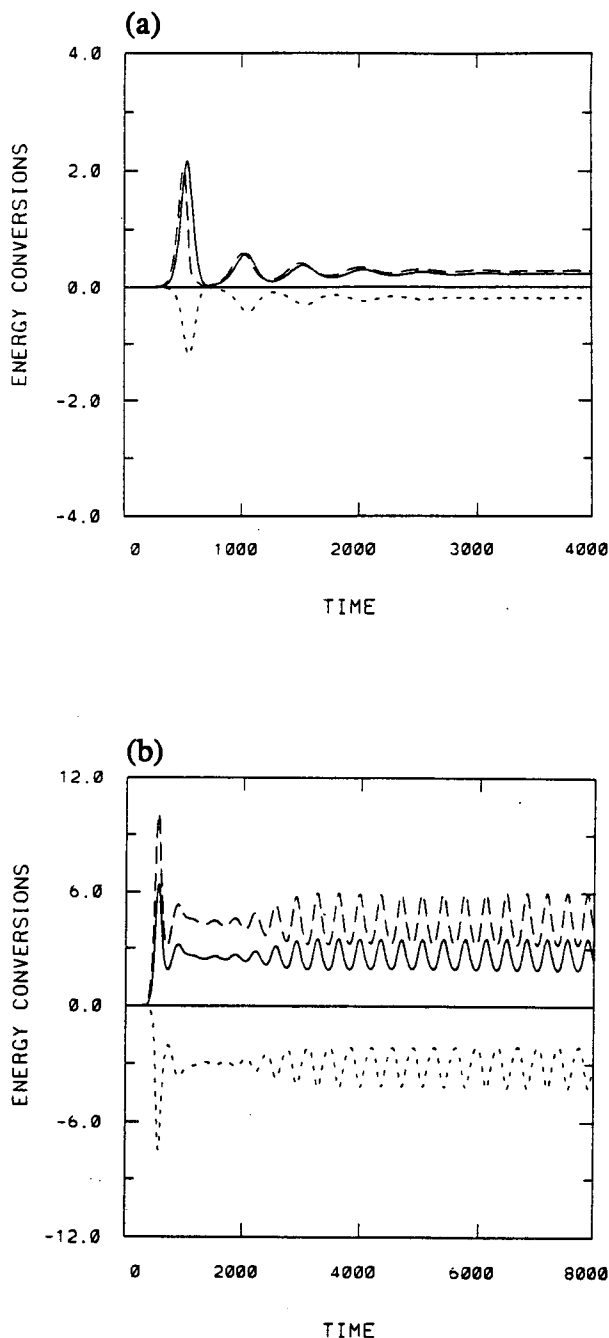


FIG. 6. Eddy energy (multiplied by  $2.0 \times 10^3$ ) and energy conversion (multiplied by  $1.0 \times 10^5$ ) for the wide limit  $\sigma = 16.0$  westerly jet; (a)  $r_f = r_t$ , (b)  $r_f = 10r_t$ . Solid line denotes total disturbance energy; long dashed line, baroclinic conversion; short dashed line, barotropic conversion.

model. Based on the energetics shown in Fig. 6, a plausible explanation for this behavior is that the surface friction increases the vertical tilt of the disturbance, which in turn allows the disturbance to grow to a larger

energy via baroclinic processes. In addition, as the disturbance grows, the enhanced vorticity fluxes increase the meridional shear of the zonal wind and increase the effectiveness of the barotropic governor. However, the barotropic governor cannot overcome the stronger baroclinic energy conversion. Furthermore, it is interesting to note that because of the large increase in  $c_r$  in the  $r_f = 10r_l$  case, a critical layer never forms in the lower layer. Even though a critical layer fails to form, strong mixing still takes place in the center of the lower layer at a time shortly after the disturbance reaches its first total energy maximum since  $\partial Q_2 / \partial y$  goes to zero in that region. In all of the other examples in this study, both with and without surface Ekman friction and for both the wide and narrow jet limits, a critical layer always develops in the lower layer.

## 5. Conclusions

In this study, numerical integrations were performed with the two-layer quasigeostrophic model to examine the properties of the wave-mean flow interaction during baroclinic life cycles. Two cases were considered: a wide and a narrow jet limit. These limits were constrained by the requirement that the instability of these jets lead to realistic baroclinic life cycles characterized by baroclinic growth and barotropic decay. Scaling arguments that resemble those of Andrews and McIntyre (1976) were used to explain the nonlocal (local) properties of the zonal-wind tendency for wide (narrow) jet limits. As a result, it was shown that both narrow and wide jet scaling can apply to realistic baroclinic life cycles in the two-layer model. Timing differences for the acceleration of the jet center were found for the two cases. For the wide jet, this acceleration was limited to the growth stage, whereas for the narrow jet it takes place during both the growth and decay stages of the life cycle. These differences were shown to be related to the timing of the lower-layer potential vorticity fluxes that force the acceleration of the jet. In addition, for both the wide and narrow jet limits, irreversible potential vorticity mixing occurs both in the center of the lower layer and at the wings of the jet in the upper layer. As a result, this mixing must drive the nonlocal and local permanent changes to the zonal wind for the wide and narrow jets, respectively. A comparison was also made as to whether the potential vorticity flux or the vorticity flux is a better predictor of the zonal-wind tendency. It was argued that in the wide (narrow) jet limits, the vorticity (potential vorticity) flux does better at predicting the zonal-wind tendency.

Last, it was shown that the foregoing inviscid (excluding horizontal diffusion) properties are retained in numerical integrations with thermal forcing and surface Ekman friction. With the thermal forcing fixed and the surface Ekman friction varied, the total disturbance energy was found to increase (decrease) with the Ek-

man friction coefficient in the wide (narrow) jet limit. However, the increase in total disturbance energy for the wide jet limit was shown to arise from baroclinic processes and not by the barotropic governor mechanism of James and Gray (1986).

The results of this study suggest a two-layer extension of the barotropic model of Held and Phillips (1987). They find acceleration at the center of the jet in the region of excitation and deceleration at the wings of jet where the disturbance is absorbed. In the two-layer model, the jet is also accelerated in the region of excitation and decelerated in the disturbance absorption region. However, in the two-layer model, these regions occur in different layers as the excitation (absorption) region is located at the center (wings) of the jet in the lower (upper) layer. In addition, in the wide jet limit for the two-layer model, there is a nonlocal zonal-wind response, which of course is not present in a barotropic model.

The model calculations also suggest that it is possible to use a barotropic model to study the temporal evolution of the upper-layer flow for both the narrow and wide jet limits. In the narrow jet limit, the disturbance must be externally forced. Otherwise, in contrast to the results presented in subsection 3b, the upper-layer jet would be accelerated throughout the life cycle. This forcing represents the generation of disturbance potential enstrophy due to the poleward meridional heat flux, which of course cannot be represented in a barotropic model. On the other hand, in the wide jet limit, an initial-value approach (as in Held and Phillips 1987) can be adopted. In this case, it is not necessary to represent the meridional heat flux by an external forcing because the meridional heat flux cancels when the upper- and lower-layer meridional potential vorticity fluxes are summed (recall from subsection 3c that the upper-layer zonal-wind tendency is closely approximated by the sum of the upper- and lower-layer potential vorticity fluxes, which in turn is well approximated by the upper-layer vorticity flux). These differences in the barotropic representation for the narrow and wide jet limits just reflect the local and nonlocal zonal-wind tendencies, respectively, for these two limiting cases.

Additional insight into the properties of the meridional radiation of the disturbance can be obtained by examining the upper-layer vorticity flux. For the wide jet limit, as discussed in the previous paragraph, the upper-layer vorticity flux is very similar to the upper-layer zonal wind tendency. By viewing Fig. 2a, and relating the upper-layer vorticity flux to the meridional radiation of the disturbance, it can be seen that the radiation from the center of the jet is completed during the growth stage and that this radiation is confined to the wings of the jet during the decay stage. For the narrow jet limit, the upper-layer vorticity flux closely resembles the upper- (lower-) layer potential vorticity

flux at the wings (center) of the jet (the upper-layer vorticity flux and lower-layer potential vorticity flux at the center of the jet are similar because in this region the lower potential vorticity flux is dominated by the meridional heat flux, and, as stated in subsection 3b, the upper-layer vorticity flux and meridional heat flux are almost identical). Thus, to visualize the upper-layer vorticity flux for the narrow jet limit, we must sum the potential vorticity fluxes in Fig. 3c and 3d. By looking at these figures, we can see, in contrast to the wide jet limit, that the disturbance is radiating in the meridional direction throughout the entire life cycle.

The results of this study show that the lower-layer potential vorticity mixing contributes to the maintenance of the westerly jet. In the narrow jet limit, the mixing maintains the lower-layer jet against surface friction. On the other hand, in the wide jet limit, this mixing acts together with surface friction [see Eq. (13)] in the lower layer and thermal forcing in the upper layer to maintain the jet in both layers. With regard to the atmosphere, these results suggest that surface mixing associated with frontogenesis contributes to the maintenance of the midlatitude westerly jet. Such a relationship between surface processes and maintenance of the midlatitude westerly jet have been discussed by Hoskins (1983) and Pfeffer (1987), who show that a poleward surface heat flux induces a thermally direct residual circulation. Further studies are planned with a primitive equation model to investigate this link between surface frontogenesis, baroclinic life cycles, and the maintenance of the westerly jet.

*Acknowledgments.* The computations for this study were performed on the Cray X-MP 2/8 supercomputer of the Ontario Center for Large Scale Computation at the University of Toronto. I would like to thank two anonymous reviewers, whose helpful comments sig-

nificantly improved this paper. In addition, I'd like to thank Drs. Isaac Held, Theodore Shepherd, and Sukyoung Lee for their helpful comments.

#### REFERENCES

- Andrews, D. G., and M. E. McIntyre, 1976: Planetary waves in horizontal and vertical shear, the generalized Eliassen-Palm relation and the mean zonal acceleration. *J. Atmos. Sci.*, **33**, 2031-2048.
- Charney, J. G., and P. G. Drazin, 1961: The dynamics of long waves in a baroclinic westerly current. *J. Geophys. Res.*, **66**, 83-109.
- Feldstein, S. B., 1991: A comparison of the weakly nonlinear instability of westerly and easterly jets in a two-layer beta-plane model. *J. Atmos. Sci.*, **48**, 1701-1717.
- , and I. M. Held, 1989: Barotropic decay of baroclinic waves in a two-layer beta-plane model. *J. Atmos. Sci.*, **46**, 3416-3430.
- Haynes, P. H., and T. G. Shepherd, 1989: The importance of surface-pressure changes in the response of the atmosphere to zonally-symmetric thermal and mechanical forcing. *Quart. J. Roy. Meteor. Soc.*, **115**, 1181-1208.
- Held, I. H., and P. J. Phillips, 1987: Linear and nonlinear barotropic decay on the sphere. *J. Atmos. Sci.*, **44**, 200-207.
- Hoskins, B. J., 1983: Modelling of the transient eddies and their feedback on the mean flow. *Large-Scale Dynamical Processes in the Atmosphere*. B. J. Hoskins and R. P. Pearce, Eds., Academic Press, 169-199.
- James, I. N., 1987: Suppression of baroclinic instability in horizontally sheared flows. *J. Atmos. Sci.*, **44**, 3710-3720.
- , and L. J. Gray, 1986: Concerning the effect of surface drag on the circulation of a baroclinic planetary atmosphere. *Quart. J. Roy. Meteor. Soc.*, **112**, 1231-1250.
- Pfeffer, R. L., 1987: Comparison of conventional and transformed Eulerian diagnostics in the troposphere. *Quart. J. Roy. Meteor. Soc.*, **113**, 237-254.
- Randel, W. J., and J. L. Stanford, 1985a: An observational study of medium-scale wave dynamics in the Southern Hemisphere summer. Part I: Wave structure and energetics. *J. Atmos. Sci.*, **42**, 1172-1188.
- , and —, 1985b: The observed life cycle of a baroclinic instability. *J. Atmos. Sci.*, **35**, 1364-1373.
- Simmons, A. J., and B. J. Hoskins, 1978: The life cycles of some nonlinear baroclinic waves. *J. Atmos. Sci.*, **35**, 414-432.
- , and —, 1980: Barotropic influences on the growth and decay of non-linear baroclinic waves. *J. Atmos. Sci.*, **37**, 1679-1684.